



TABLE 1

Chemical composition of tested materials

	Chemical composition (wt. %)															
	C	Mn	Si	P	S	Cr	Ni	W	Mo	Cu	V	Ti	Fe	Mg	Zn	Ti+Zr
304L	0.05	1.35	1.0	0.016	0.008	18.58	17.3	0.025	0.02	0.04	0.03	0.013	bal.	–	–	–
PA6	–	0.65	0.64	–	–	0.03	0.01	–	–	4.23	–	0.04	0.35	0.75	0.18	0.04

one, thus, it is necessary to take into account both the heat transfer within the specimen and the heat exchange between the specimen and the surroundings. Thus, the objective of this work is to specify the threshold above which, for tested materials and given experimental conditions, the non-uniform temperature distribution can be properly used as the indicator of plastic strain localization.

2. Experimental procedure

2.1. Specimen preparation

The experiments were performed on austenitic stainless steel 304L and aluminium alloy (PA6) with chemical compositions shown in Table 1.

The specimens were cut out from sheets using electro-erosion machining. The shape and dimensions of the specimen is presented in Fig. 1. Then, surface of the specimens were electro polished in order to obtain mirror-like, stress free surfaces.

On the one side of the gauge part of the specimen a markers in form of dots were painted (Fig. 2). The other side was covered by soot to ensure high and uniform emissivity of the surface (soot emissivity ~0.95).

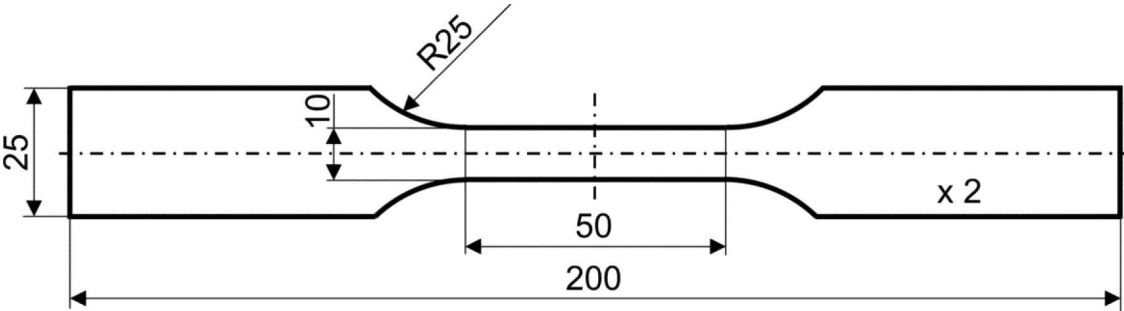


Fig. 1. Shape and dimensions of the specimen

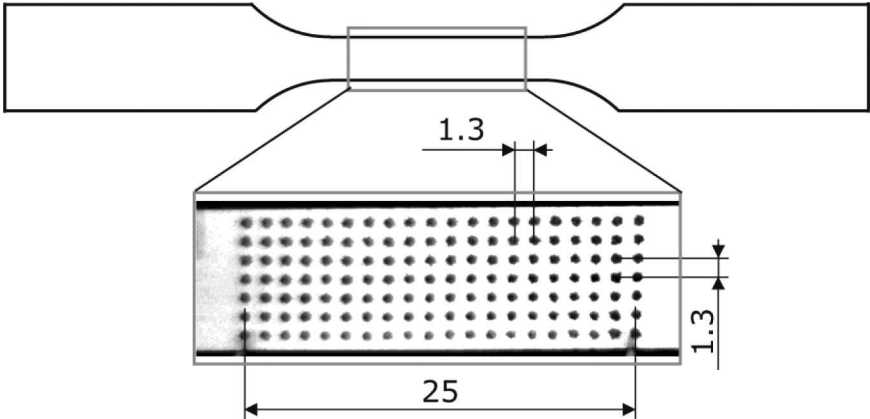


Fig. 2. Markers in form of dots placed on the one side of gauge part of the specimen

## 2.2. Determination of strain and temperature fields

Such prepared specimens were strained using MTS 858 testing machine with different displacement rates: 100 mm/min, 1000 mm/min and 2000 mm/min. There was no insulation between specimen and the grips. During straining the sequence of images was recorded using CCD visible light camera. On the basis of recorded sequence, the displacements of markers centres were determined.

Knowing the initial distance between centres of dots  $l_0$  and current distance between the centres as a function of deformation time  $l(t)$ , the local true strain  $\varepsilon(t)$  in tensile direction was calculated:

$$\varepsilon(t) = \ln \left( \frac{l(t)}{l_0} \right). \quad (1)$$

Simultaneously the opposite side of the specimen was observed using IR thermographic system and surface distribution of the temperature as a function of deformation time was recorded.

## 2.3. Determination of the onset of plastic strain localization

On the basis of obtained strain and temperature fields the onset of plastic strain localization was determined. The analysis was limited to the markers laying on the specimen axis (Fig. 3). The strains  $\varepsilon(t)$  were calculated for each neighbouring dot centres as a function of deformation time. The mean temperature was calculated for all segments between centres of markers (see Fig. 3). Taking into account the accuracy of both methods (spatial resolution, thermal sensitivity, surface uniformity, etc.), the threshold values of true strain and mean temperature difference corresponding to the plastic strain localization were established. The values of true

strain and temperature difference higher than 0.01 and  $1^\circ\text{C}$ , respectively, were assumed as indicators of plastic strain localization. It means that from that point the deformation starts to be non-homogeneous.

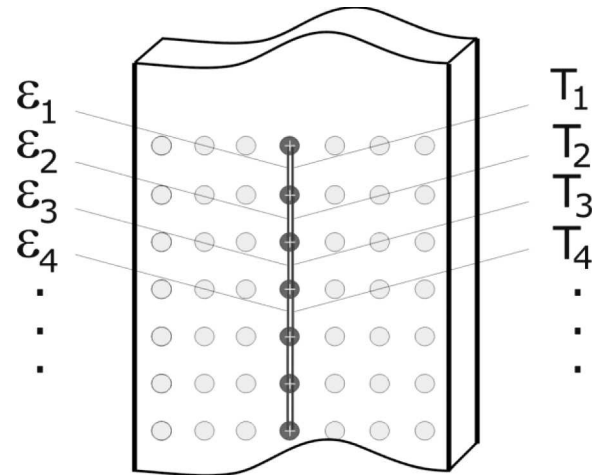


Fig. 3. Schematic diagram showing the position of markers for which true strain and mean temperature were determined

## 3. Results

On the basis of time dependences of strain and temperature, the onset of plastic strain localization was determined. In Figs. 4a-6a the true strain vs. time dependences for austenitic steel strained at displacement rates: 100 mm/min, 1000 mm/min and 2000 mm/min, are presented. It is seen that initially the deformation is homogeneous and then different areas of specimen deform in different rates. The points lying in the area of strain localization deform much faster than that lying outside of the localized zone. In all figures the point where strain difference  $\Delta\varepsilon$  is greater than 0.01 are marked as the onset of strain localization.

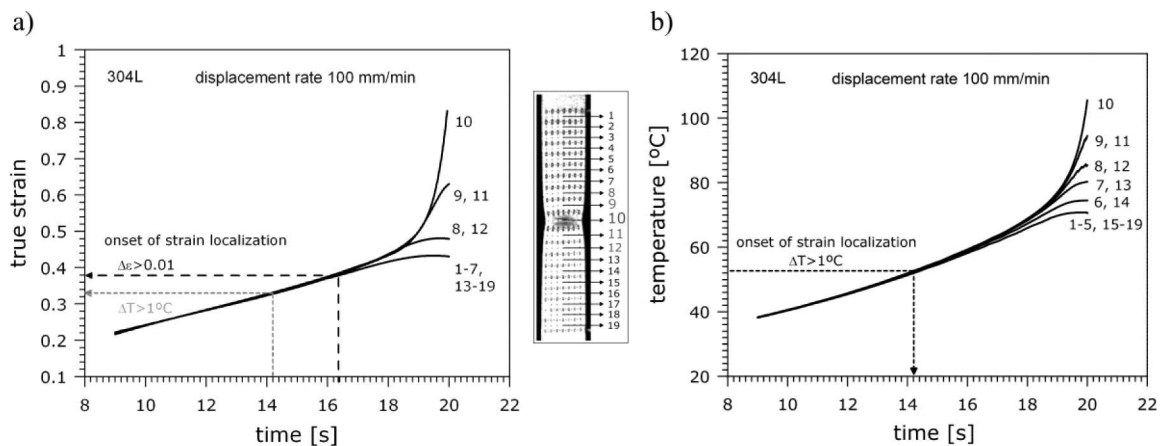


Fig. 4. The dependence of true strain a) and mean temperature b) vs. deformation time for austenitic steel strained at displacement rate 100 mm/min. The onsets of strain localization corresponding to  $\Delta\varepsilon > 0.01$  and  $\Delta T > 1^\circ\text{C}$  are marked

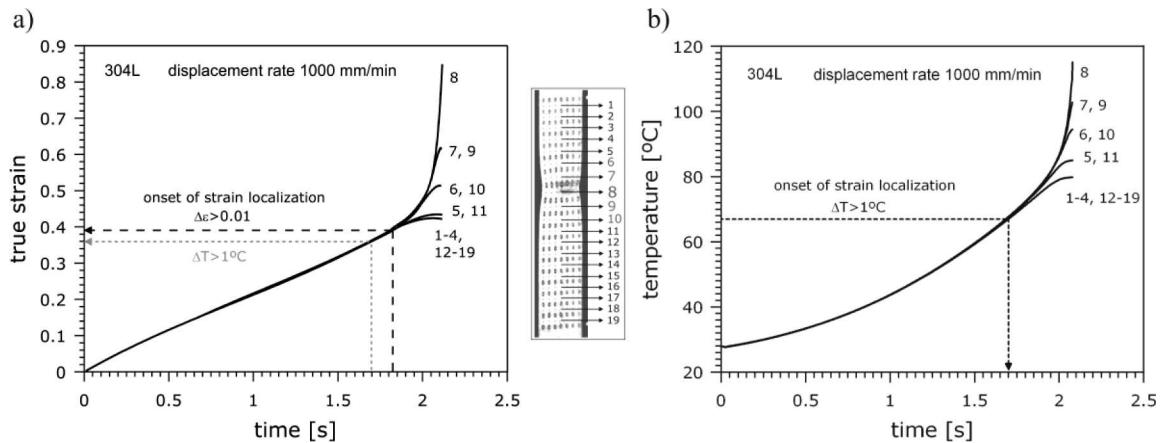


Fig. 5. The dependence of true strain a) and mean temperature b) vs. deformation time for austenitic steel strained at displacement rate 1000 mm/min. The onsets of strain localization corresponding to  $\Delta\epsilon > 0.01$  and  $\Delta T > 1^\circ\text{C}$  are marked

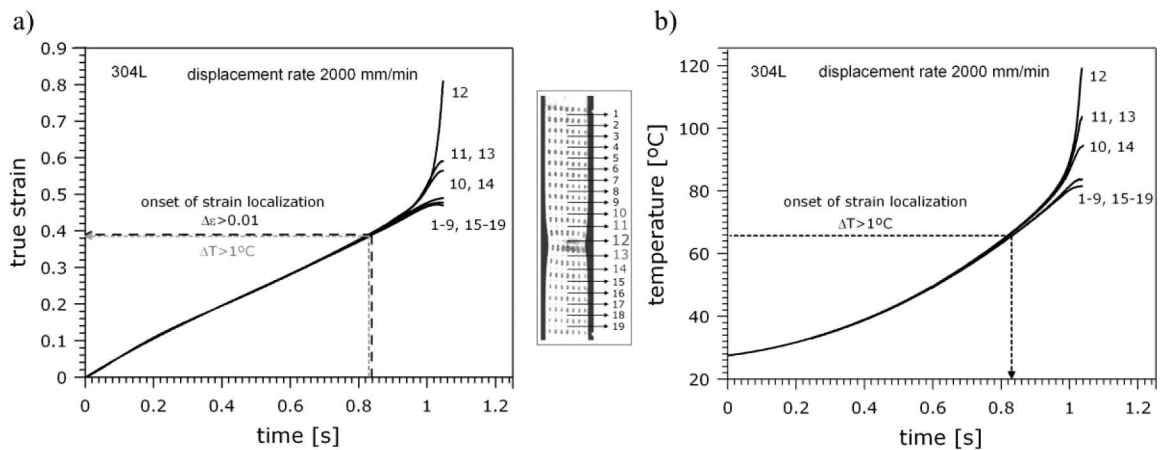


Fig. 6. The dependence of true strain a) and mean temperature b) vs. deformation time for austenitic steel strained at displacement rate 2000 mm/min. The onsets of strain localization corresponding to  $\Delta\epsilon > 0.01$  and  $\Delta T > 1^\circ\text{C}$  are marked

In Figs.: 4b-6b the mean temperature vs. time dependences for austenitic steel strained at same displacement rates are presented. As in case of strain vs. time dependence, the thermal response is initially homogeneous and then become non-homogeneous. In all figures the points, where the mean temperature difference  $\Delta T$  is greater than  $1^\circ\text{C}$ , are marked. On the basis of time corresponding to those points, the values of strain corresponding to the onset of strain localization were found from true strain vs. time dependence (see Figs.: 4a-6a). In Table 2 the comparison of strain values obtained using both methods is presented. It is seen, that for 100 mm/min the value of strain corresponding to the onset of plastic strain localization determined on the basis of strain field ( $\Delta\epsilon > 0.01$ ) is equal to 0.38, whereas that obtained using temperature field ( $\Delta T > 1^\circ\text{C}$ ) is equal to 0.33 (see Fig. 4a and 4b). This means that, for this displacement rate the heat transfer within the specimen and the heat exchange between the specimen and the surroundings are significant and should not be neglected. In other words,

for these experimental conditions, non-uniform temperature distribution could not be used as an indicator of the onset of plastic strain localization. It is seen that the increase of displacement rate to 1000 mm/min is still not sufficient. In this case, obtained values of strain corresponding to the onset of strain localization for strain and temperature fields are equal 0.39 and 0.36, respectively (see Fig. 5a and 5b). The increase of displacement rate up to 2000 mm/min cause that results obtained using both methods are almost the same (see Fig. 6a and 6b). It means that the deformation process is carried out fast enough to neglect heat transfer within the specimen and between the specimen and the surroundings.

In Figs.: 7-9 the true strain and mean temperature vs. time for aluminium alloy strained at displacement rates: 100 mm/min, 1000 mm/min and 2000 mm/min, are presented. In Table 3 the comparison of strain values corresponding to the onset of plastic strain localization, obtained using both methods are presented. It is seen that, as in case of austenitic steel, the non-uniform

temperature distribution can be used as an indicator of plastic strain localization from displacement rate equal to 2000 mm/min.

TABLE 2

The comparison of strain values corresponding to the onset of plastic strain localization, obtained on the basis of strain and temperature fields for austenitic steel

	Displacement rate [mm/min]	Onset of strain localization $\Delta\varepsilon > 0.01$	Onset of strain localization $\Delta T > 1^\circ\text{C}$
304L	100	0.38	0.33
	1000	0.39	0.36
	2000	0.39	0.39

TABLE 3  
The comparison of strain values corresponding to the onset of plastic strain localization, obtained on the basis of strain and temperature fields for aluminium alloy

	Displacement rate [mm/min]	Onset of strain localization $\Delta\varepsilon > 0.01$	Onset of strain localization $\Delta T > 1^\circ\text{C}$
PA6	100	0.15	0.12
	1000	0.16	0.14
	2000	0.15	0.15

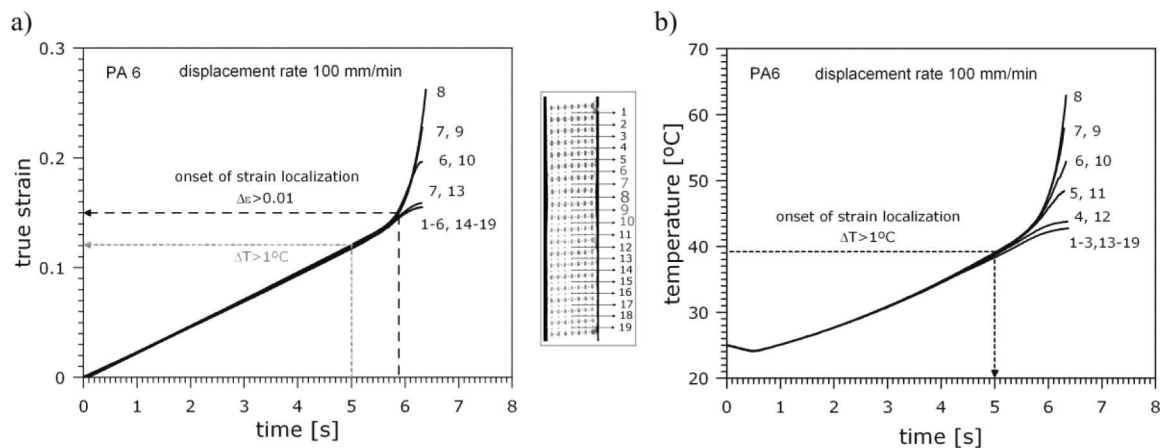


Fig. 7. The dependence of true strain a) and mean temperature b) vs. deformation time for aluminium alloy strained at displacement rate 100 mm/min. The onsets of strain localization corresponding to  $\Delta\varepsilon > 0.01$  and  $\Delta T > 1^\circ\text{C}$  are marked

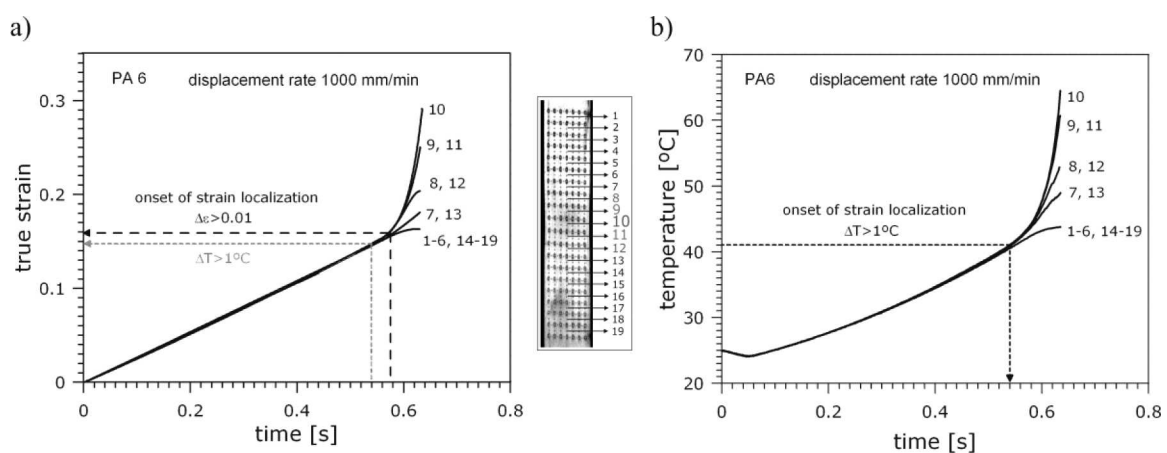


Fig. 8. The dependence of true strain a) and mean temperature b) vs. deformation time for aluminium alloy strained at displacement rate 1000 mm/min. The onsets of strain localization corresponding to  $\Delta\varepsilon > 0.01$  and  $\Delta T > 1^\circ\text{C}$  are marked



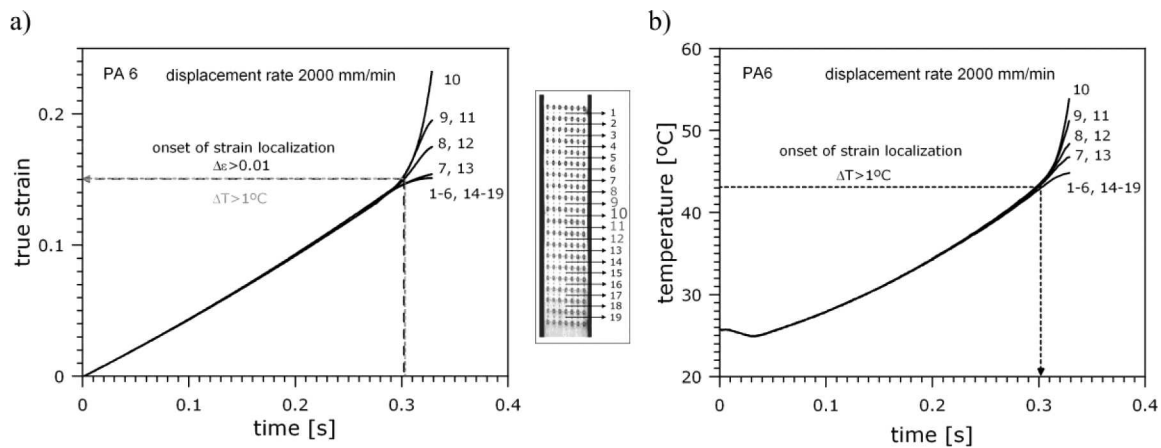


Fig. 9. The dependence of true strain a) and mean temperature b) vs. deformation time for aluminium alloy strained at displacement rate 2000 mm/min. The onsets of strain localization corresponding to  $\Delta\epsilon > 0.01$  and  $\Delta T > 1^\circ\text{C}$  are marked

#### 4. Concluding remarks

The onset of plastic strain localization was determined using two independent methods based on strain and temperature field analysis. Specimens were strained at different displacement rates: 100 mm/min, 1000 mm/min and 2000 mm/min, in order to find the limit, above which both methods give similar results. In other word, to find a limit when, the heat transfer within the specimen and between specimen and the surroundings can be neglected. It has been shown that initially the deformation is homogeneous and than become non-homogeneous. It has been shown that in case of both tested materials, the displacement rate 2000 mm/min can be treated as a limit, above which the non-uniform temperature field can be used as an indicator of plastic strain localization.

#### REFERENCES

- [1] A.K. Ghosh, *Metall. Trans.* **5**, 1607-1616 (1974).
- [2] P.V. Makarov, *Theor. Appl. Fract. Mec.* **33**, 23-30 (2000).
- [3] B. Wattrisse, A. Chrysochoos, J.-M. Muracciole, M. Némoy-Gaillard, *Eur. J. Mech. A-Solid.* **20**, 189-211 (2001).
- [4] W.Y. Chien, J. Pan, S.C. Tang, *Int. J. Plasticity* **20**, 1956-1981 (2004).
- [5] F. Lagattu, J. Brillaud, M.-C. Lafarie-Frenot, *Mater. Charact.* **53**, 17-28 (2004).
- [6] J.J. Lopez Cela, I. Munoz Diaz, *Comput. Struct.* **83**, 1824-1833 (2005).
- [7] T.S. Byun, N. Hashimoto, *Nucl. Eng. Technol.* **38**, 619-638 (2006).
- [8] B. Guelorget, M. Francois, C. Vial-Edwards, G. Montay, L. Daniel, J. Lu, *Mat. Sci. Eng. A-Struct.* **415**, 234-241 (2006).
- [9] A. Holger, *Int. J. Plasticity* **23**, 789-840 (2007).
- [10] G. Montay, M. Francois, M. Tourneix, B. Guelorget, C. Vial-Edwards, I. Lira, *Opt. Laser. Eng.* **45**, 222-228 (2007).
- [11] S.-H. Tung, M.-H. Shih, J.-C. Kuo, *Opt. Laser. Eng.* **48**, 636-641 (2010).
- [12] A. Chrysochoos, H. Louche, *Int. J. Eng. Sci.* **38**, 1759-1788 (2000).
- [13] H. Louche, A. Chrysochoos, *Mater. Sci. Eng. A-Struct.* **307**, 15-22 (2001).
- [14] B. Wattrisse, J.-M. Muracciole, A. Chrysochoos, *Int. J. Therm. Sci.* **41**, 422-427 (2002).
- [15] W. Oliferuk, M. Maj, *Mater. Sci. Eng. A-Struct.* **387-389**, 218-221 (2004).
- [16] B. Yang, P.K. Liaw, M. Morrison, C.T. Liu, R.A. Buchanan, J.Y. Huang, R.C. Kuo, J.G. Huang, D.E. Fielden, *Intermetallics* **13**, 419-428 (2005).
- [17] W. Oliferuk, M. Maj, *Mater. Sci. Eng. A-Struct.* **462**, 363-366 (2007).
- [18] W. Oliferuk, M. Maj, *Arch. Metall. Mater.* **52**, 2, 250-256 (2007).
- [19] B. Berthel, A. Chrysochoos, B. Wattrisse, A. Galtier, *Exp. Mech.* **48**, 79-90 (2008).
- [20] A. Rusinek, J.R. Klepaczko, *Mater. Design* **30**, 35-48 (2009).
- [21] O.A. Plekhov, O.B. Naimark, *J. Appl. Mech. Tech. Phy.* **50**, 127-136 (2009).
- [22] S. Dumoulin, H. Louche, O.S. Hopperstad, T. Břrvik, *Eur. J. Mech. A-Solid.* **29**, 461-474 (2010).
- [23] W. Oliferuk, M. Maj, R. Litwinko, L. Urbanski, *Eur. J. Mech. A-Solid.* **35**, 111-118 (2012).